NASA TECHNICAL NOTE

NASA TN D-4295

STRUCTURAL FEASIBILITY STUDY OF PRESSURIZED TANKS FOR LIQUID-METHANE FUELED SUPERSONIC AIRCRAFT

by Rene E. Chambellan, Joseph F. Lubomski, and William A. Bevevino

Lewis Research Center
Cleveland, Ohio

NATIONAL AERONAUTICS AND SPACE ADMINISTRATION • WASHINGTON, D. C. • DECEMBER 1967

STRUCTURAL FEASIBILITY STUDY OF PRESSURIZED TANKS FOR LIQUID-METHANE FUELED SUPERSONIC AIRCRAFT

By Rene E. Chambellan, Joseph F. Lubomski, and William A. Bevevino

Lewis Research Center
Cleveland, Ohio

NATIONAL AERONAUTICS AND SPACE ADMINISTRATION

For sale by the Clearinghouse for Federal Scientific and Technical Information
Springfield, Virginia 22151 – CFSTI price $3.00

STRUCTURAL FEASIBILITY STUDY OF PRESSURIZED TANKS FOR LIQUID-METHANE FUELED SUPERSONIC AIRCRAFT

by Rene E. Chambellan, Joseph F. Lubomski, and William A. Bevevino

Lewis Research Center

SUMMARY

Light-weight pressurized tanks for the storage of liquid-methane fuel in the wings of supersonic transport aircraft were evaluated. Three types of tank structures were studied: (1) membrane tanks where the only loads in the tank skin are tensile, (2) modified semimonocoque tanks composed of a framework of rings and stringers covered by a pressure-tight skin, and (3) filamentary restrained membrane tanks where the outer skins of either metal or sealed fabric are restrained by wires or threads attached to the opposite skin. A typical wing void space having an approximately rectangular prismoidal shape was assumed as a tank envelope.

The various tank designs were compared by the use of two numerical ratios, namely, the volumetric efficiency and tank-weight to contained-fuel-weight ratio. Volumetric efficiency is defined as the ratio of the volume of fuel stored in the tank to the storage void volume into which the tank is fitted. For the designs considered, exclusive of insulation, volumetric efficiencies ranged from 81.1 to 99.6 percent and tank-weight to contained-fuel-weight ratios ranged from 0.0241 to 0.0556.

No single tank design considered proved to be superior with respect to both volumetric efficiency and the ratio of tank weight to contained fuel weight. For the situation where there is inadequate storage volume for fuel and where it becomes necessary to redesign the airplane, detailed tank designs and aircraft range and payload analyses will be required to determine the proper compromise between tank weight and volumetric efficiency. Based on volumetric efficiency alone the best design is the tridirectional filamentary restrained membrane tank. This tank is composed of six flat faces restrained by three sets of orthogonally placed internal filaments. When the tank-weight to contained-fuel-weight ratio is the only criterion, then the single-lobe unidirectional filamentary restrained membrane configuration is the best design. This single-lobe tank has two flat opposed faces connected by filaments, and the remaining four sides of the tank are closed by semicylinders.

INTRODUCTION

Liquid methane, because of its high heat of combustion and large heat-sink capacity, shows considerable promise as a fuel for supersonic transport aircraft. The investigation evaluates the weight and volumetric efficiency of several concepts of nonintegral pressurized tanks for containing liquid methane in supersonic aircraft wings. A study of the use of liquid methane as a fuel for a Mach 3 commercial supersonic transport airplane showed that a payload improvement of up to 31 percent and a reduction in direct operating costs of 36 percent might be realized (ref. 1). These reported advantages are based on the assumption that the higher specific volume of liquid methane would not materially alter the specific tank weight. Therefore, weight penalties associated with the storage of liquid-methane fuel on board the airplane will establish, to a considerable extent, whether or not the anticipated gains can be obtained.

At standard atmospheric pressure, liquid methane boils at -258.5° F (111.76° K) and has a specific weight of 25.9 pounds per cubic foot (414.9 kg/m^3) which is about one half the specific weight of JP fuel. Consequently, a very efficient tank insulation system would be required and the total on-board storage volume necessary would be large when compared with the requirements for JP fuel.

Conventional aircraft designs, using tanks designed for JP fuel, require that the pressure in the fuel tanks decrease as aircraft altitude increases. Permitting this to occur with a cryogenic fuel could result in an intolerable rate of boiloff during climb. This boiloff is due to the lowered boiling point at lower pressures. Conversely, if the tank internal pressure were permitted to maintain ambient atmospheric pressure by venting as the aircraft altitude decreased, the fuel would become subcooled. A further hazard in venting to atmosphere is the possibility of permitting a combustible mixture of air and methane vapor to form in the ullage space. If the tank pressure were not permitted to increase as the aircraft descended from altitude, a tank crushing pressure could result, because the vapor pressure of the liquid methane would be less than the ambient atmospheric pressure. One method of circumventing these problems is to use fuel tanks pressurized to, or higher than, 1 atmosphere (1×10^5 N/m^2).

Ideally, a cryogenic fuel should be stored in large volume tanks with low tank-wall surface area to volume ratio, such as can be obtained within an airplane fuselage. Since volume in an efficient supersonic transport type aircraft is quite limited, the low density of liquid methane would probably require storage of part of the fuel in the wing where surface to volume ratios would be less favorable than in the fuselage.

This investigation was conducted to determine the relative merits of several types of pressurized nonintegral wing tanks for storing liquid methane on board a supersonic transport. Three types of tank structures were studied, namely,

(1) Membrane tanks, where the only loads in the tank skin are tensile
(2) Modified semimonocoque tanks, composed of a framework of rings and stringers covered by a pressure-tight skin
(3) Filamentary restrained membrane tanks, where the outer skins of either metal or sealed nonmetallic fabric are restrained by wires or threads that traverse the tank interior and are attached to the opposite skin

The various tanks have been compared on the basis of weight and volumetric efficiency for internal pressure levels of 15 and 30 psig (10.343 and 20.685 N/cm^2). The wing void assumed for tank installation is a trapezoidal prismoid 88 inches (2.235 m) long, 16 inches (0.4064 m) wide, and with depths of 21.5 inches (0.5461 m) and 28.5 inches (0.7239 m) at either end.

SELECTION OF TANK TYPES

Tank Pressurization

Liquid methane, under controlled pressure, can be stored on board the aircraft in integral tanks or in nonintegral tanks. The second alternative allows higher tank pressures. Integral tanks, in general, cannot withstand a pressure differential across the skin of more than 4 psig (2.758 N/cm^2); thus, if saturated liquid methane (at standard atmospheric conditions) is stored on board the airplane, methane will boil off as a consequence of reduced ambient pressure as the airplane gains altitude. One method for reducing the boiloff problem is to use subcooled methane in integral tanks. The amount of subcooling that could be specified would depend on the availability of subcooled liquid methane at a reasonable cost and the results of a trade-off study of the relative costs of other such factors as boiloff loss and insulation requirements. Another consideration would be the determination of the feasibility of maintaining a controlled pressure in the tank ullage space with a nonsoluble, noncondensible, pressurant gas. The need for a pressurant gas over the subcooled liquid methane is to prevent the reduction of tank internal pressure, since the vapor pressure of a subcooled fluid is less than ambient standard atmospheric pressure. Depending on the degree of subcooling, the tank internal pressure could drop enough to imperil the tanks by the presence of an external crushing pressure. Finding a suitable pressurant gas presents some difficulties. Nitrogen is soluble in subcooled liquid methane up to 10 percent by weight and, as reported in reference 1, would cause such a weight penalty that the indicated advantages to be gained from the higher heating value of methane over that of conventional JP fuels would be largely nullified. Helium, hydrogen, or superheated methane could be used as pressurant gases over subcooled liquid methane. The use of superheated methane gas has a disadvantage in that

sloshing of the subcooled liquid methane could result in sudden condensation of the methane gas. Unless sufficient additional superheated methane gas were introduced in a timely manner, a crushing pressure on the aircraft tanks could result. The use of hydrogen gas as a pressurant introduces problems concerning safety because of its wide flammability limits and low required ignition energy. Helium could be used as a pressurant; however, its relative scarcity raises questions of economy and availability.

One way of eliminating boiloff losses of liquid methane, incurred in going to higher altitudes, is to maintain sufficient pressure in the fuel tanks. From practical considerations of ground handling and storage, the assumption has been made that commercially available liquid methane would be at the boiling point at a pressure of 1 atmosphere. The severity of the boiloff problem due to reduced pressure is described in reference 1 for a supersonic transport airplane having a takeoff fuel weight of about 200 000 pounds (90 720 kg). The boiloff results from reduced tank pressure due to increasing airplane altitude. Four minutes after takeoff, the boiloff becomes equal to the engine requirements, and, from this time to about $8\frac{1}{2}$ minutes after takeoff, the boiloff rates exceed engine fuel consumption requirements. During the $4\frac{1}{2}$-minute interval just considered, the boiloff exceeds the fuel consumption of the engine by 2000 pounds (907.2 kg) (1.0 percent of total fuel load), and the total boiloff without subcooling amounts to 19 100 pounds (8664 kg) (9.5 percent of total fuel load).

A further consideration exists here in that the boiloff vapors are not readily useable as engine fuel. The utilization of boiloff would require compression of the fuel vapor, which imposes a high power requirement, and a weight penalty due to compressor weight. Furthermore, a complication exists in that a two-phase-fuel metering and pumping system would be required.

Boiloff loss and the inability of the airframe to sustain high internal pressures were the primary reasons for orienting this study toward nonintegral pressurized tank designs.

In the comparison of integral and nonintegral tanks, two different sets of problems become apparent. (1) With integral tanks a large portion of available storage space can be utilized, but problems exist in establishing adequate insulation systems capable of withstanding pressure loads and/or high temperatures on the outer surface and remaining leakproof and minimizing heat shorts to the airframe. Wing structures of conventional design are not intended to withstand internal pressures of more than about 4 psig (2.758 N/cm^2); therefore, it is not practical to consider pressurized integral tanks, as this would cause severe weight penalties on the aircraft. (2) For nonintegral, pressurized tanks the airframe structural problems are reduced. Problems of tank fastening, insulation, light-weight design, and effective utilization of available storage space remain.

Insulation

The use of liquid methane in an actual aircraft requires the use of insulation systems to reduce heat flow into the fuel and prevent frost formation on the external surfaces of the aircraft. Insulation weights and volumes were not accounted for in these analyses. To incorporate consideration of insulation systems requires further studies of various factors such as weight, volume, fuel boiloff, and cost to obtain an optimum fuel storage system. The insulation system for integral tanks must be exposed to the liquid; therefore, the insulation must be considered as either wet or dry. Dry insulation must withstand compressive loads and have a surface which is impervious to fuel leaks. A wet insulation (ref. 2) permits fluid to come in contact with the inner surface of the tank wall and thus absorb heat from the wall. This fluid then vaporizes and, as a consequence of the close packing of the insulation material, the vapor is inhibited from flowing back into the bulk fluid. Thus the trapped vapor becomes a part of the insulation system, eliminating the concern for a leak-proof insulation.

Insulation materials can be readily applied to the external surfaces of nonintegral tanks thus simplifying the insulation problem over that which would exist if the internal surfaces of a tank were to be insulated. Insulation applied to the external surface of a nonintegral tank can be more easily inspected, is not subject to crushing pressures, and is not subject to wetting by the fuel, thereby making it superior, in these respects, to insulation applied to the internal surfaces of the tank.

Tank Types and Shapes

In the selection of wing tank designs, a supersonic transport aircraft configuration, having a large internal wing volume for fuel storage, was assumed. A wing design with this feature would probably have voids of approximately rectangular prismoidal shape (fig. 1). Horizontal cross sections of storage voids are rectangles and spanwise vertical

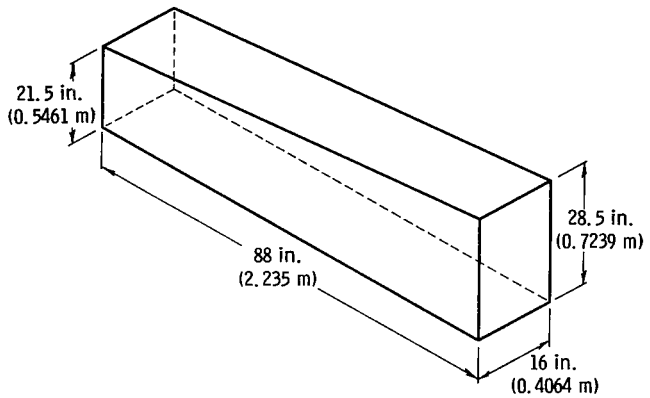

Figure 1. - Typical configuration of wing void space.

cross sections are trapezoidal. These geometric constraints preclude the use of tanks of simple configuration.

Three types of tanks are reported herein, namely, a conventional membrane type (hereinafter called "membrane", fig. 2), a modified semimonocoque type (hereinafter called "semimonocoque", fig. 3), and an internal filamentary restrained membrane type

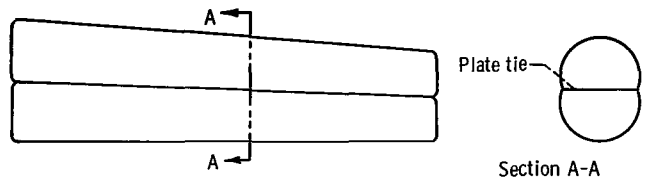

(a) Two-lobe design.

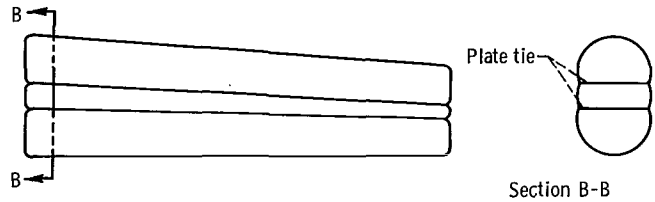

(b) Three-lobe design.

Figure 2. - Membrane tank designs.

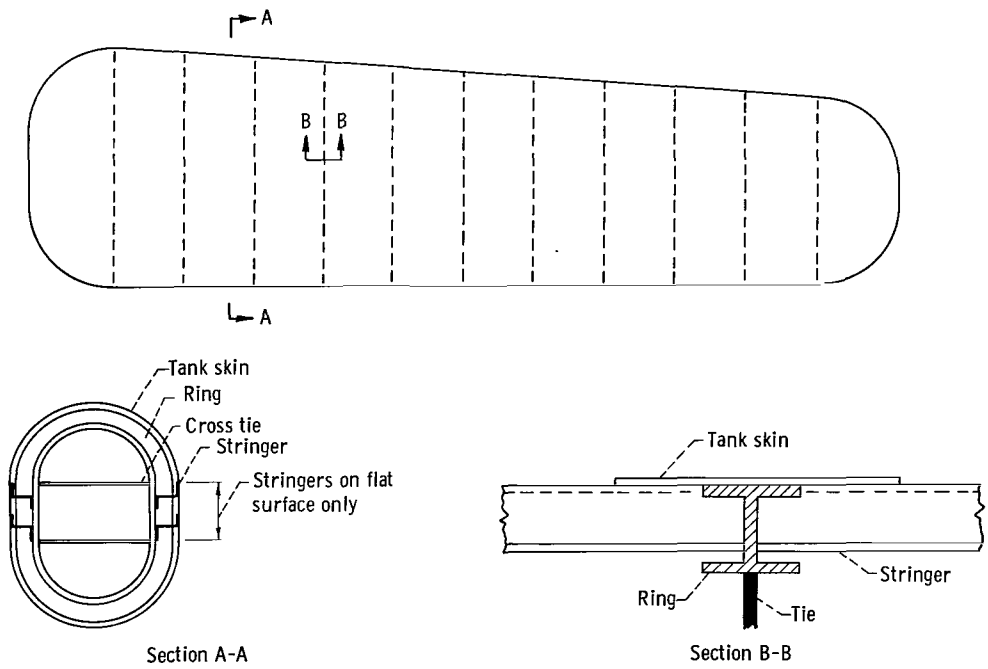

Figure 3. - Modified semimonocoque tank with rounded closures.

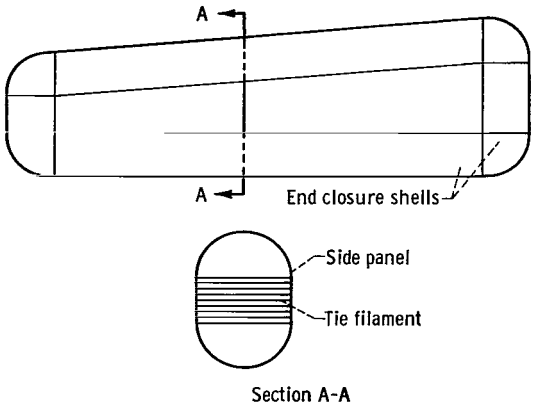

(a) One-lobe configuration.

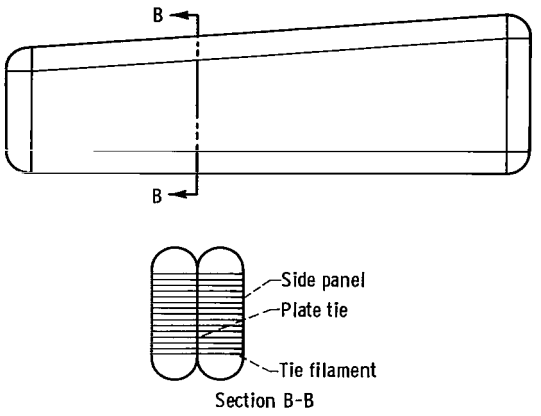

(b) Two-lobe configuration.

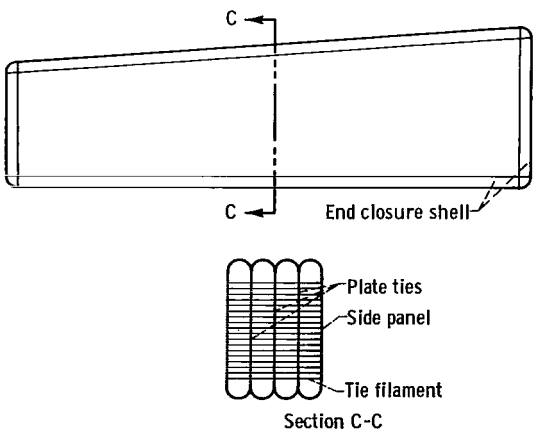

(c) Four-lobe configuration.

Figure 4. - Unidirectional filamentary restrained membrane tanks.

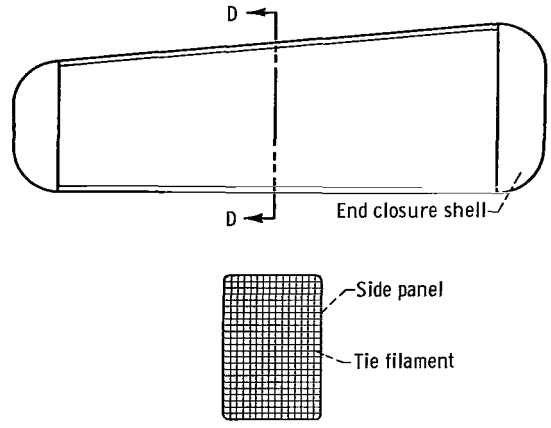

(a) Bidirectional configuration.

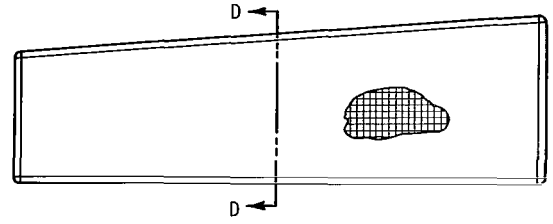

(b) Tridirectional configuration.

Figure 5. - Bidirectional and tridirectional filamentary restrained membrane tanks.

(hereinafter called "filament tank", figs. 4 and 5). A membrane tank resists internal pressure by the action of tensile stresses in the tank walls. In multilobe-membrane tanks metal tie sheets are introduced to balance loads at lobe intersections. The semimonocoque tank is composed of a skin covered system of restrained rings with or without stringers and resembles a squared off airplane fuselage. The use of stringers is dependent on whether or not reinforcement of the tank skin in the longitudinal direction is needed. To reduce bending moments carried by the rings, restraints on the rings can be used. The filament tank is composed of flat opposed faces connected together by numerous internal tie threads or wires, fastened in a direction approximately perpendicular to the faces. If only two flat faces are used then the ends would be enclosed with semicylinders of the same materials as the faces, which then intersect at the corners (fig. 4(a)). If a system or orthogonal internal ties are used, then the other faces of the tank can also be flat (fig. 5). When the tank is pressurized internally, the ties are stretched in restraining the faces. This pressurized tank is stable and can carry external loads.

ANALYTICAL PROCEDURES

Assumptions

In the design study the following assumptions were made:

(1) The wing void space into which the fuel tank must fit is a prismoidal volume with a width of 16 inches (0.4064 m), a length of 88 inches (2.235 m), and heights of 21.5 inches (0.5461 m) at one end and 28.5 inches (0.7239 m) at the other end (fig. 1). This void is considered to be typical for the wing of a large supersonic transport aircraft.

(2) The tanks are internally pressurized, and two pressure differentials between tank internal pressure and tank external pressure are considered. These pressure differentials are 15 and 30 psi (10.343 and 20.685 N/cm^2).

(3) The tank material is a titanium alloy with the following mechanical properties:

Yield stress, σ_y, psi^2; N/m^2	150 000; 103 425
Shear yield stress, τ_y, psi; N/m^2	90 000; 62 055
Specific weight, ω, lb/in^3; kg/m^3	0.160; 0.4429
Modulus of elasticity, E, psi; N/cm^2	17.0×10^6; 11.72×10^6

(All symbols are defined in appendix A.)

(4) A minimum allowable material thickness of 0.010 inch (0.0254 cm) is assumed.

(5) Any insulation requirement is assumed to be accounted for by increases in the tank void space dimensions. Furthermore, no reinforcement of the tanks by insulation is assumed.

(6) The allowable working stress is one third of the material yield stress.

Structural Methods

Membrane tanks. - These tanks are subjected to predominately membrane stresses. Stresses are computed according to membrane theory and the calculation is shown in appendix B. The tie plates are perforated to maintain stress in the tie plates equal to the stress in the tank wall.

Semimonocoque tanks. - For the design of these tanks the tank skin located between the stringers and rings was analyzed as a membrane clamped at all edges. For the tank configuration without stringers the skin between rings was analyzed as a membrane clamped at two edges. The spacing of the rings and stringers was varied until the stress of the skin was equal to the allowable stress of the skin material. With the spacing of the rings and stringers determined, the size of these components was established. The stringers were considered as uniformly loaded beams, simply supported, and the rings

were analyzed as rings subjected to a uniformly distributed in-plane loading.

A simplified analysis was performed for the purpose of producing a preliminary design for the tank. To obtain an optimum tank design a more exact analysis would be required. Such an analysis would require the solution of equations for a highly redundant structure. The analysis used in the design of the modified semimonocoque tank is presented in appendix C.

Filament tanks. - An idealized structure was assumed for determining the working stresses in these configurations where four structural components were isolated as free bodies (appendix D). These components are

(1) Tie filament

(2) End closure shells

(3) Plate ties (in the two- and four-lobe tanks)

(4) Side panels

Each tie filament supports a tensile load, proportional to the area of the side panel restrained by the tie filament. The closures at the tank ends and at the top and bottom of the tanks are analyzed as membranes. In the unidirectional filament tank configurations for either the two- or four-lobe design, the tie plates are subjected to a biaxial plane stress due to loads from the closures. These plates are sized by proportioning the plate cross-sectional net area to maintain the allowable working stress. If the tie plate stresses are below the allowable working stress, the tie plate cross-sectional area can be reduced by perforating the plate, beyond that required for passage of tie filaments, thus, reducing weight.

A conservative analysis was used to calculate the working stresses in the side panels. The structural element under consideration here is a square plate restrained at the corners by the tie threads and subjected to a uniform pressure on one side with tensile edge loads on all four edges. Several approximations were made to obtain an estimate of stress distributions in the panels (appendix D).

RESULTS AND DISCUSSION

Tank Characteristics

In this study several characteristics pertinent to a comparison of various tank designs, which are applicable to a typical wing void space, were evaluated. The tank characteristics determined were the volumetric efficiency, tank weight, and tank weight to contained-fuel-weight ratio (or tank- to fuel-weight ratio). Volumetric efficiency is the ratio of the net internal volume of the tank to the net internal volume of the wing void space. The void shape, previously described as a prismoidal volume, has a lengthwise vertical projection which is a trapezoid with a length of 88 inches (2.235 m), end

TABLE I. - COMPARISON OF VARIOUS TANK CONFIGURATIONS FOR TYPICAL STORAGE VOLUME

Tank type	Tank pressure								Refer to figure -
	15 psig (10.343 N/cm^2)				30 psig (20.685 N/cm^2)				
	Volumetric efficiency, percent	Tank weight		Tank weight to contained fuel weight ratio	Volumetric efficiency, percent	Tank weight		Tank weight to contained fuel weight ratio	
		lb	kg			lb	kg		
Single-lobe, unidirectional filamentary restrained membrane (one-lobe tank)	81.8	10.40	4.72	0.0241	81.8	11.07	5.02	0.0256	4(a)
Double-lobe, unidirectional filamentary restrained membrane (two-lobe tank)	91.1	14.99	6.8	0.0312	91.1	16.37	7.43	0.0341	4(b)
Quadruple-lobe, unidirectional filamentary restrained membrane (four-lobe tank)	95.6	20.08	9.11	0.0397	95.6	21.82	9.9	0.0432	4(c)
Bidirectional filamentary restrained membrane (bidirectional tank)	93.0	14.36	6.51	0.0292	93.0	17.96	8.15	0.0366	5(a)
Tridirectional filamentary restrained membrane (tridirectional tank)	99.6	16.75	7.6	0.0322	99.5	23.40	10.61	0.044ᵕ	5(b)
Nonmetallic fabric filamentary restrained membrane (fabric tank)	81.8	12.16	5.52	0.0282	81.8	23.98	10.88	0.0556	4(a)
Modified simimonocoque (semimonocoque tank)	81.7	13.74	6.23	0.0318	81.7	17.98	8.16	0.0417	3
Conventional membrane (membrane tank)	81.1	11.87	5.38	0.0279	81.1	11.87	5.38	00279	2

heights of 21.5 inches (0.546 m) and 28.5 inches (0.7239 m), and vertical end projections which are rectangles each 16 inches (0.4064 m) wide with end heights of 21.5 inches (0.5461 m) and 28.5 inches (0.7239 m), respectively (fig. 1). The characteristics for the tanks were determined for internal pressures of 15 and 30 psig (10.343 and 20.685 N/cm^2) and are shown in table I. To facilitate comparison of the various tank designs, data from table I is also shown in bar chart form in figures 6 and 7. The effect of insulation thickness is not considered or included in these data.

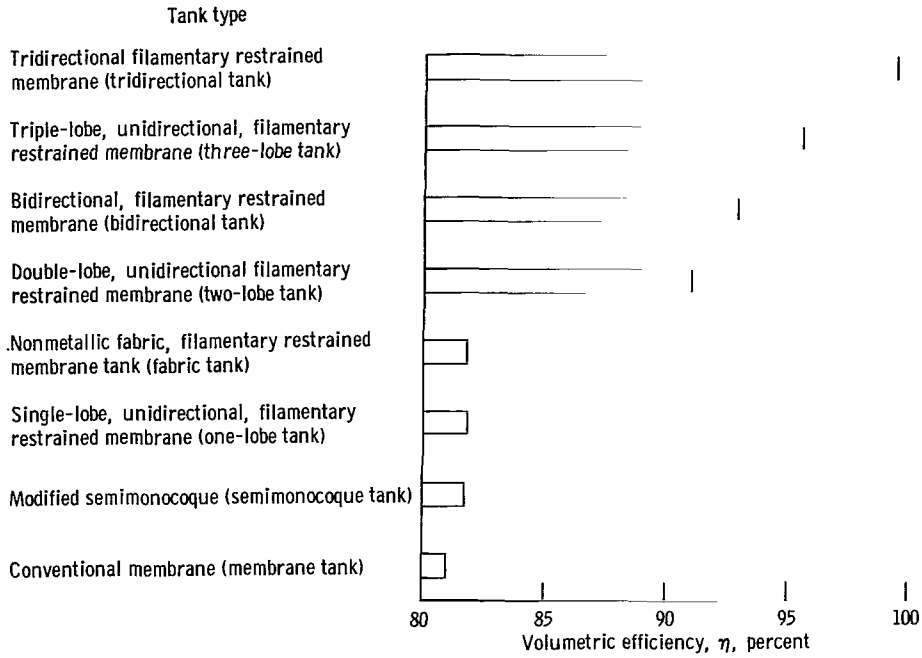

Figure 6. - Comparison of various tank designs based on volumetric efficiency.

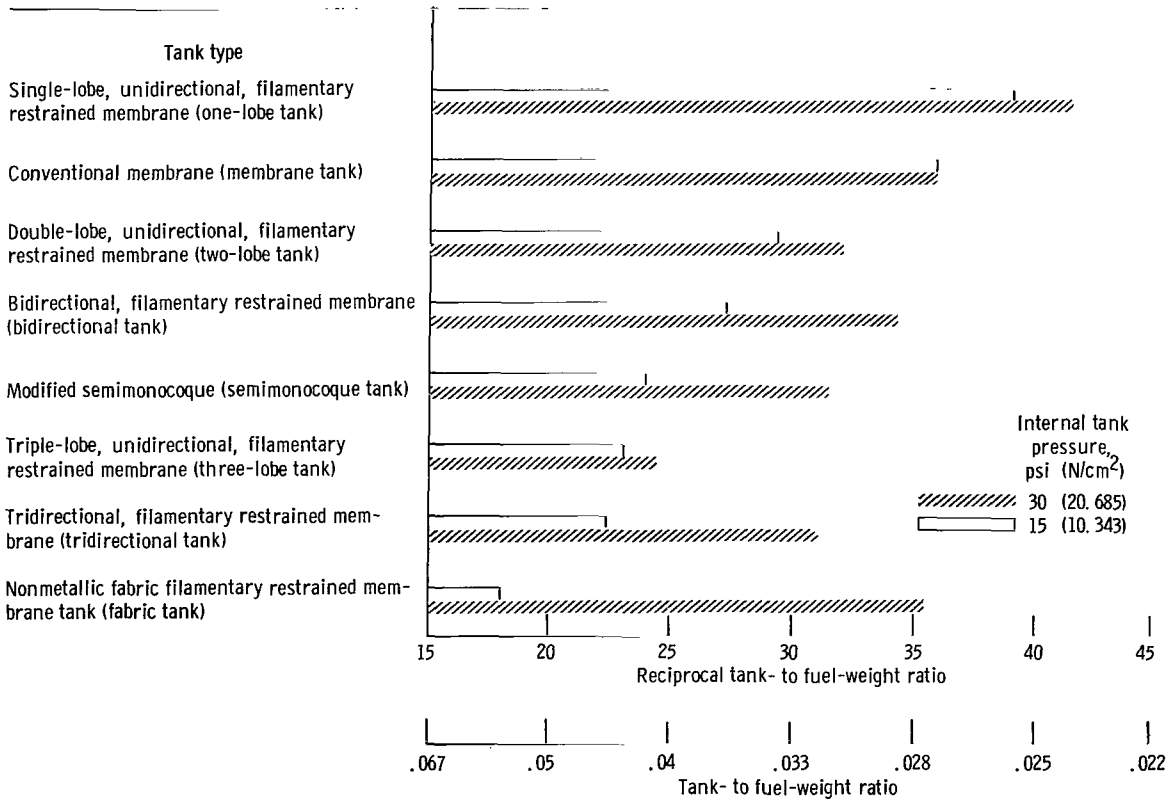

Figure 7. - Comparison of various tank designs based on the tank- to fuel-weight ratio for two tank pressures.

Perusal of table I reveals that the highest volumetric efficiency is obtained with the tridirectional filamentary restrained membrane tank (hereinafter called tridirectional tank) which utilizes approximately 99.5 percent of the available volume. For the configurations considered, the lower volumetric efficiencies are realized with the single-lobe unidirectional filamentary restrained tanks (hereinafter called "one-lobe tank"), the nonmetallic fabric filamentary restrained membrane tank (hereinafter called "fabric tank"), the semimonocoque tank, and the membrane tank. The volumetric efficiencies for these four tanks are almost identical. This result is expected since the tank configurations are very similar. For all the configurations considered, the volumetric efficiency is virtually independent of tank pressure.

Further inspection of table I shows that, as expected, tank weight is a function of tank internal pressure, except for the membrane design where its weight is independent of pressure. This is because the 0.010-inch (0.0254-cm) minimum tank skin gage results in stresses much lower than the maximum allowable. For a design pressure of 15 psig (10.343 N/cm^2) the one-lobe tank is the lightest design with the membrane and fabric tanks being heavier by 14 and 17 percent, respectively, and the heaviest tank is the quadruple-lobe filamentary restrained membrane (hereinafter called "four-lobe tank"), which is 93 percent heavier than the one-lobe design. At a design pressure of 30 psig (20.685 N/cm^2) the one-lobe tank is the lightest tank with the membrane tank only $7\frac{1}{4}$ percent heavier and all the other designs are more than 48 percent heavier than the one-lobe design. These relative weight increases are due to the fact that some of the tank designs require the addition of material to keep working stresses below the allowable maximum stress when the design pressure is increased from 15 to 30 psig (10.343 to 20.685 N/cm^2). The membrane tank designed with the minimum gage titanium sheet and pressurized to 30 psi (20.685 N/cm^2) produces a membrane stress which is 50 percent of the assumed maximum allowable working stress. A minimum wall thickness of 0.010 inch (0.0254 cm) for the tanks was selected because practical considerations of handling would make tanks built of thinner material highly susceptible to damage.

The weight changes in the filament tanks are due to the increase of tie filament diameter from 0.020 to 0.030 inch (0.0508 to 0.0762 cm). This increase in tie filament diameter is required to keep the working stress of the tie filament below the assumed allowable stress. The weight increases are directly related to the number of tie wires; therefore, the multidirectional tanks are more severely affected than the unidirectional tanks. The weight increase of the one-lobe and the tridirectional tank, due to a change in pressure from 15 to 30 psi (10.343 to 20.685 N/cm^2), is 6.5 and 39.8 percent, respectively. The semimonocoque design which has rings as the major structural element is designed so that the rings react in bending to the applied pressure loading. Increasing the tank internal pressure from 15 to 30 psig (10.343 to 20.685 N/cm^2) requires an increase in tank weight of 30.8 percent. The weight of the fabric tank increases 97.1 per-

cent when the internal pressure is raised from 15 to 30 psig (10.343 to 20.685 N/cm^2). This weight increase, based on empirical estimates from a manufacturer, is due to the requirement for a heavier fabric and more sealant at the higher pressure. The specific strengths of the nommetallic fibers, that is, the tensile strength to specific weight ratio, is considerably greater than for metals. Therefore, it seems feasible that weights of the fabric type tank could be reduced through a concerted development effort where the fibers are used more effectively and sealant requirements are reduced.

The third characteristics shown in table I, designated tank- to fuel-weight ratio, is a measure of the effectiveness of the tank as a pressurized container. On this basis, the best tank configuration at both 15 and 30 psi (10.343 and 20.685 N/cm^2) is the one-lobe tank and the second best is the membrane tank. The respective tank- to fuel-weight ratios exclusive of insulation and other fuel-system component weight, are about 0.025 and 0.028. The tank- to fuel-weight ratio for the membrane design is greater by 15.8 and 8.9 percent than that for the one-lobe design for the pressures considered.

Comparison of the various tank designs by means of volumetric efficiency, tank weight, and tank to fuel-weight ratio reveals that no single tank design is superior in all respects, when considering the assumed reference volume. The tridirectional tank has a very high volumetric efficiency; however, its weight and its tank- to fuel-weight ratio are also high. The one-lobe tank has a relatively low volumetric efficiency; however, its tank weight and tank- to fuel-weight ratio are also low.

In a general application, consideration must be given to the overall airframe configuration. If adequate storage space is not available, then more space must be provided, resulting in additional airframe structural weight. In this case, tank designs with high volumetric efficiencies might be preferable even though the weight penalty is higher. However, if storage volume availability is not critical, then the tank designs possessing low tank- to fuel-weight ratios would be chosen. Before proceeding further into considerations for providing pressurized nonintegral tanks to a generalized wing void space, it is necessary to evaluate the effects on the three tank characteristics caused by variations in the proportions of the tank storage void space.

Tank Designs

Results shown in table I are for tanks fitted to a definite storage void. In the following discussion the variations of the tank characteristics as the tank storage void is changed are considered. Specifically the variations in characteristics are considered for changes in width and depth of the tank. The effect of end closures on the characteristics is made negligible by assuming that the length of the tank is very long so that the effect of the end closures on volumetric efficiency is negligible. This is tantamount to assuming that the characteristics are a function of the tank cross section only.

A generalized storage void, in the shape of a rectangular parallelopiped, with a width of a, which is also the maximum width of the tank configuration, is assumed. The storage void height h, which is also the maximum tank height, is equal to Na. The cross-sectional area of the storage void is a rectangular shape having a cross-sectional area Na^2. Using these parameters, calculations were made expressing the volumetric efficiency as a function of N and the tank- to fuel-weight ratio as a function of N and a for several configurations.

Membrane Tank (Two and Three Lobes)

As is seen from figure 8 the volumetric efficiency has a maximum value for both the three- and two-lobe membrane tank. For the double-lobe membrane tank, the volumetric

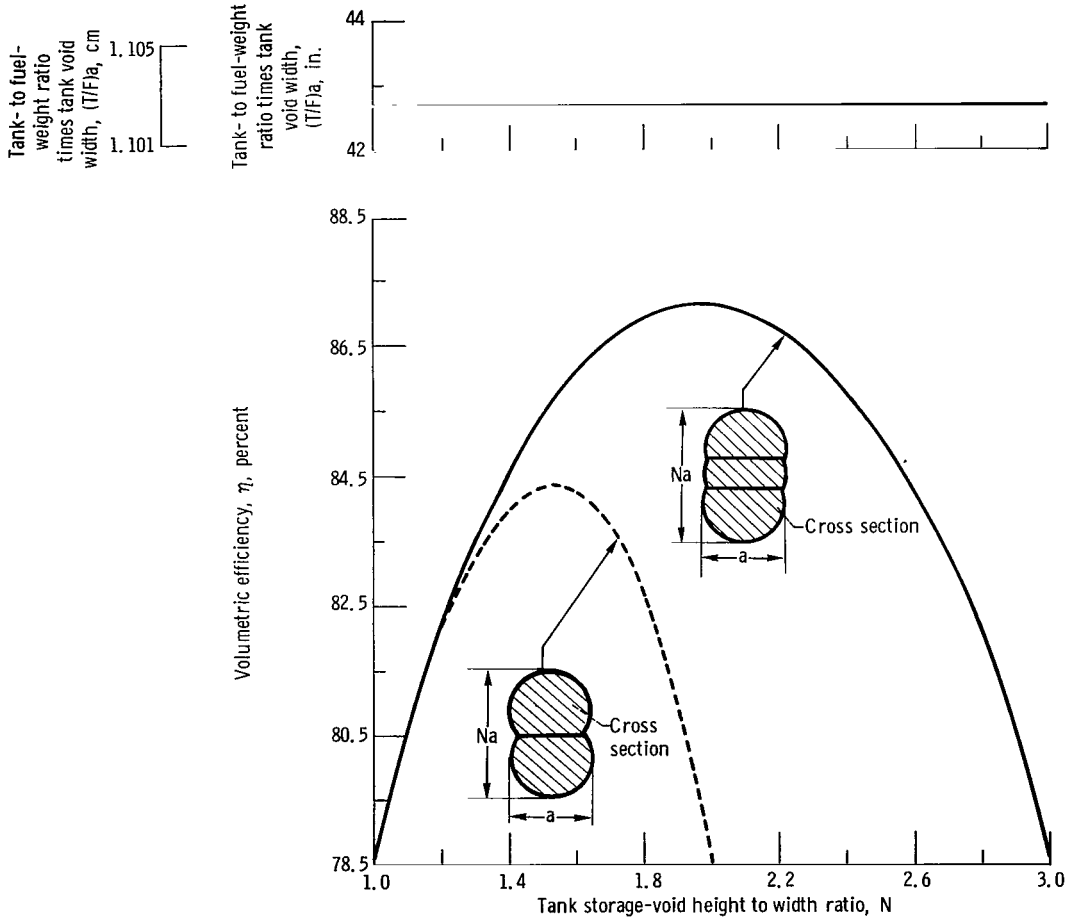

Figure 8. - Volumetric efficiency and tank- to fuel-weight ratio as function of tank storage-void height to width ratio for titanium membrane tank of unit length with 0.010-inch (0.0254-cm) skin thickness and filled with liquid methane.

efficiency has a maximum value of 84.3 percent for a value of N of about 1.5 The largest practical value of N for the two-lobe configuration is two. For the three-lobe membrane configuration. which has the largest practical value of N = 3, a maximum volumetric efficiency if 87.1 percent occurs at a value of N = ≈ 2.0. For both these configurations, the volumetric efficiency is independent of a, for values of $t/a \ll 1/4$ and a function of N only. On the other hand, the tank- to fuel-weight ratio is a function of a, and independent of N. The material thickness used for tanks shown in figure 2 is 0.010 inch (0.0234 cm), and the cross-sectional area of the tie plates is adjusted to make the tensile stress in the plates equal to the hoop stress. The use of this size material limits the magnitude of a; that is, a cannot exceed a value that would cause the membrane hoop stress to exceed the allowable working stress of 50 000 psi (34 475 N/cm^2). For a tank pressure of 30 psig (20.685 N/cm^2), a can be as large as 33.3 inches (0.8458 m), for a material thickness of 0.010 inch (0.0254 cm), as determined by the following equation:

$$a = \frac{2t\sigma_a}{p}$$

One parameter plotted in figure 8 is the tank- to fuel-weight ratio multiplied by a. The tank- to fuel-weight ratio is determined by equation (B8), and this ratio multiplied by a is 0.427 inch (1.086 cm) for both tank configurations for all values of N where $t/a \ll 1/4$. To obtain the actual tank- to fuel-weight for a specific value of a, the value plotted must be divided by the value of a.

Multilobe Membrane Tanks

The equations developed in appendix C for the membrane tank express the relations for volumetric efficiency and tank weight to fuel weight ratio as functions of the tank geometry and proportions. In the foregoing discussion long tanks with two and three lobes were considered, whereas here, the scope is extended to include the effect of increasing the number of lobes. It is obvious that increasing the number of lobes k for a given tank height to tank width ratio N will increase volumetric efficiency (fig. 8). Equation (B6) gives the relation between N and k for maximizing volumetric efficiency. For N = 1 and k = 1 the void cross section is square and the tank cross section is a circle. Equation (B6) is valid for all other positive values of N and k, and for tank design purposes k must be an integral value and satisfy the condition $k \geqq N$. For values of k up to and including k = 9, values of N satisfying equation (B6) were calculated, and, for these values of N and the corresponding value of k, the volumetric efficiency was computed

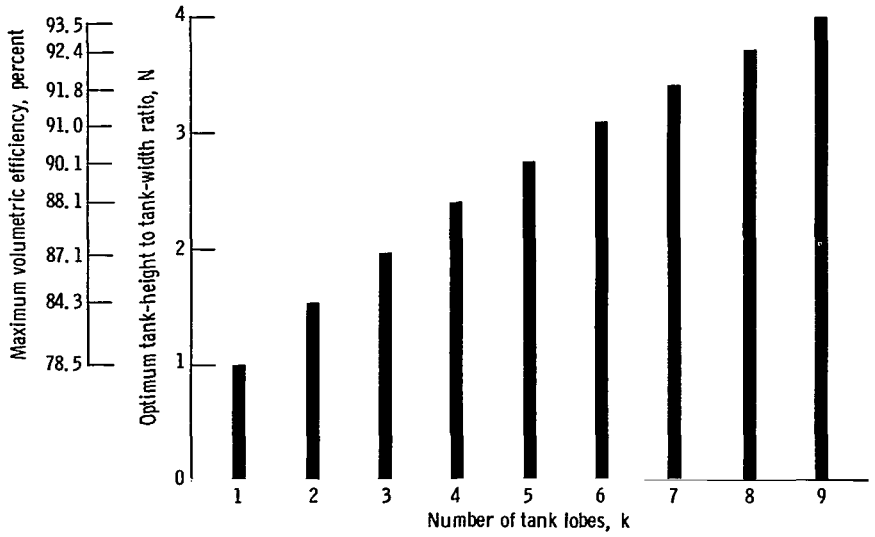

Figure 9. - Relation between tank height to tank width ratio and number of tank lobes when volumetric efficiency is maximized.

from equation (B5). This value of volumetric efficiency is the greatest value that can exist for the particular number of lobes in the design. The results obtained from these calculations are presented in figure 9. This figure shows the maximum volumetric efficiency and the corresponding tank height to tank width ratio that results in maximum volumetric efficiency for particular values of k.

The values of maximum volumetric efficiency and ratio of tank height to tank width shown on figure 9 are the same values that would be obtained at the peak of the curves such as shown in figure 8, if these curves were drawn for all the tank configurations (number of lobes).

Filament Tank

An evolution of the multilobed membrane tank, as the number of lobes increases to a large value, is the filament tank. This configuration is achieved by substituting for the tie plates, used in the membrane tank, a large number of small diameter wires (filaments) to carry the side pressure loads. By placing the tie wires at a small pitch, the sides of these tanks can be made to remain almost flat and parallel to the storage void sides, thus making more efficient use of the available volume. The volumetric efficiencies of five tank configurations of this type design were calculated from the equations presented in appendix B and these values are shown in figure 10. It is assumed that the storage void is very long so that the effect of end closures on volumetric efficiency is negligible. As for the conventional membrane tank, the volumetric efficiency is then independent of a and a function of N only. When the effects of end closures are neglected

the bidirectional and the tridirectional configurations have the same volumetric efficiencies, so that while five specific types of tanks were considered, only four curves appear on figure 10.

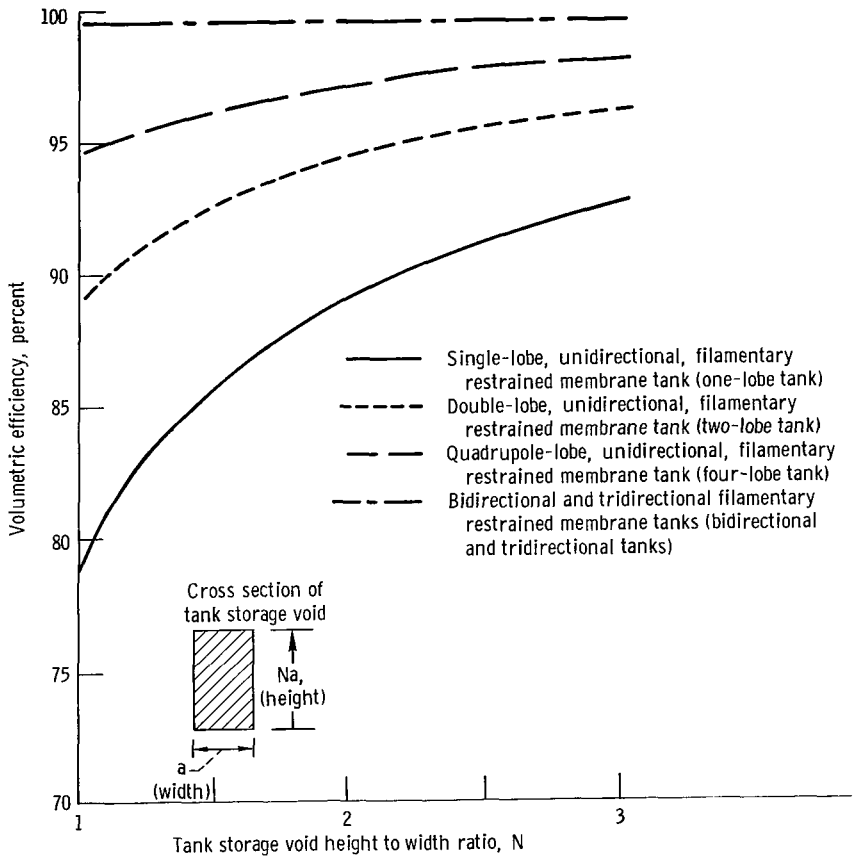

Figure 10. - Volumetric efficiency per unit tank length of filamentary restrained membrane tanks as function of tank storage-void height to width ratio.

Further examination of figure 10 shows that, for all designs considered, as N increases, the volumetric efficiency of each tank increases. If N were allowed to approach an infinite value, the volumetric efficiencies of all five configurations would approach 100 percent; however, between values of N = 1 and N = 3 there exists considerable differences between the volumetric efficiencies of the various configurations. For the range of N considered the bidirectional and the tridirectional configurations, for all practical purposes, have a constant volumetric efficiency of 99.6 percent and, while there exists a large disparity between the volumetric efficiencies of the various configurations for a storage void whose cross section is square (N = 1), the difference in volumetric efficiency diminishes as the storage void cross section height to width ratio increases. Thus for N = 1, the difference between the best volumetric efficiency, possessed by the bidirectional and tridirectional configurations, and the poorest volumetric efficiency,

possessed by the unidirectional one-lobe configuration, is 21.6 percent. At N = 3, the difference in volumetric efficiency for these configurations is only 7.6 percent.

The tank- to fuel-weight ratio multiplied by a is plotted against N for each of the five filament tanks considered and is shown in figure 11. For each tank configuration,

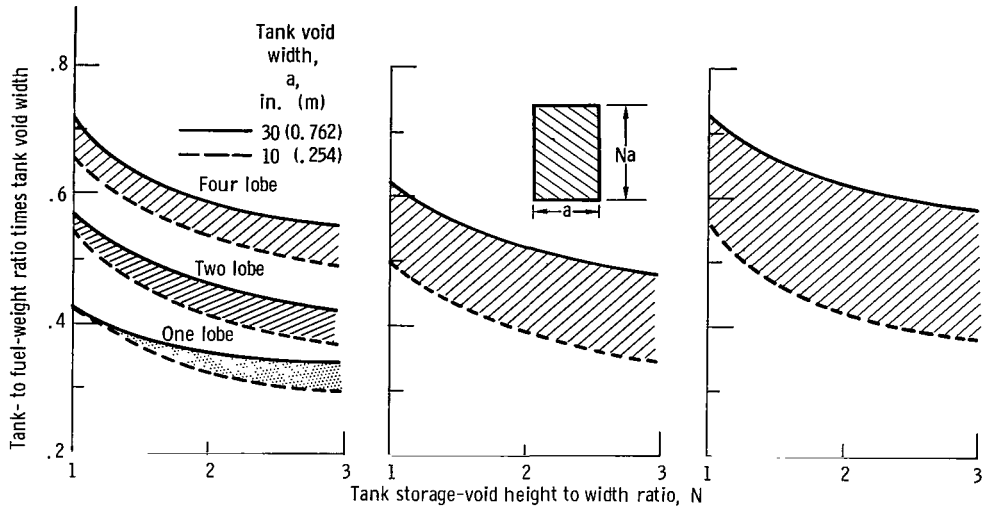

Figure 11. - Tank weight to fuel weight ratio of filamentary restrained membrane tanks as function of tank storage-void height to width ratio for tank of unit length with 0.010-inch (0.0254-cm) thick titanium skin and for widths between 10 and 30 inches (0.254 and 0.762 m), where the tanks are filled with liquid methane at pressure of 15 psig (10.343 N/cm^2).

curves are shown for a values of 10 and 30 inches (0.254 and 0.762 m). It is probable that in practical applications the majority of tank storage voids will have widths between these two values. A large difference in tank- to fuel-weight ratio is obtained for each of the configurations, but in general the shapes of the curves are similar. For a constant value of a, as the value of N increases, the tank- to fuel-weight ratio decreases. Also, for a constant value of N, as the value of a increases, the tank- to fuel-weight ratio multiplied by a increases, but the tank- to fuel-weight ratio decreases. Thus, as both a and N increase a compounded decrease in the tank- to fuel-weight ratio is possible.

The best of the five configurations studies with respect to tank- to fuel-weight ratio is the one-lobe filament tank. Considering both the effect of width a and height to width ratio N, this tank is superior to the other four because it has the lowest tank- to fuel-weight ratio. The selection of the next best configuration is somewhat more difficult. Either the two-lobe unidirectional or the bidirectional configuration is next best depending on the size and shape of the cross-sectional area of the storage void. For storage voids of about 20 inches (0.508 m) or less in width, the bidirectional configuration will yield a better tank- to fuel-weight ratio than the two-lobe unidirectional configuration regardless of the height to width ratio. But for storage voids larger than 20 inches

(0.508 m) in width the two-lobe unidirectional configuration will have the better tank- to fuel-weight ratio. The additional weight of tie wires in the larger width bidirectional tanks adversely affects the tank- to fuel-weight ratio. The tridirectional configuration is similarly affected for the larger widths. For large widths of storage void the tridirectional configuration shows a tank- to fuel-weight ratio greater than for the four-lobe tank.

Comparison of the filament configurations to the membrane tanks shows that the volumetric efficiencies of all five filament tanks are higher than that for the membrane tanks considered. The membrane-tank volumetric efficiency can be made to approach that for the one-lobe unidirectional configuration by increasing the number of lobes. For tank height to tank width ratios N less than about two, the membrane configuration is superior to all but one of the filament configurations. For N greater than two the two-lobe tank, the bidirectional tank and the tridirectional tank have lower tank- to fuel-weight ratios for narrow widths (about 10 in. or 0.254 m). As the tank height to tank width ratio increases even more, these tanks continue to improve in the intermediate width range (about 20 in. or 0.508 m).

Semimonocoque Tank

Results of analysis for the various semimonocoque tank designs considered, are presented in table II. All designs reported in table II are for the same typical wing void space as for other tank designs considered in this report. The void has a width of 16 inches (0.4064 m), a length of 88 inches (2.235 m), an average height of 25 inches (0.635 m), and a volume of 35 200 cubic inches (0.5769 cm).

In an effort to maximize volumetric efficiency, a tank design employing flat ends was first considered. The use of flat ends resulted in a high volumetric efficiency (85.7 per-

TABLE II. - SUMMARY OF DATA FOR VARIOUS SEMIMONOCOQUE CONFIGURATIONS

[Total available volume, 34 200 in.^{3} (0.576928 m^3).]

Design condition	Tank configuration	Internal tank pressure		Volume capacity of tank		Volumetric efficiency, percent	Weight of tank skin		Weight of rings		Weight of stringers		Weight of ties		Total weight of tank		Tank weight to contained fuel weight ratio
		psi	N/m^3	in.^{3}	m^3		lb	kg	lb	kg	lb	kg	lb	kg	lb	kg	
1	Flat ends	30	206.85	30 174	0.494555	85.72	9.45	4.29	11.80	26.01	4.66	2.11	----	----	40.12	18.20	0.0887
2	Spherical ends	30	206.85	28 264	.469325	80.30	9.79	4.44	9.16	20.19	3.34	1.52	----	----	33.32	15.11	.0786
3	Spherical ends	15	103.425	28 311	.464017	80.43	9.79	4.44	5.02	11.06	5.00	2.27	----	----	25.85	11.73	.0609
4	Spherical ends; ties across ring	30	206.85	28 345	.464575	80.53	9.79	4.44	1.76	3.81	3.34	1.52	3.34	1.52	20.34	9.23	.0479
5	Spherical ends; ties across ring	15	103.425	28 355	.464738	80.55	9.79	4.44	.97	2.13	5.00	2.27	1.82	.83	18.74	8.50	.0441
6	Spherical ends; ties across ring; stringers eliminated	30	206.85	28 753	.47126	81.68	10.78	4.89	1.76	3.87	----	----	3.34	1.52	17.98	8.16	.0417
7	Spherical ends; ties across ring; ties eliminated	15	103.425	28 774	.471606	81.74	9.79	4.44	.97	2.13	----	----	1.82	.83	13.74	6.23	.0318

cent for a tank pressure of 30 psig or 20.685 N/cm^2 g); however, this design also gave a large ratio of tank weight to fuel weight (table II). When spherical ends rather than flat ends are used, the volumetric efficiency is reduced by 5.4 percent and the tank- to fuel-weight ratio by 11.4 percent. When the design pressure is reduced from 30 to 15 psig (20.685 to 10.343 N/cm^{2}g) (table II, design condition 3), the tank- to fuel-weight ratio is reduced by 22.5 percent and the volumetric efficiency is virtually unchanged.

As is seen from design conditions 1, 2, and 3 (table II), the weight contribution of the rings to the total tank weight is substantial. When the rings are reinforced by cross ties, the volumetric efficiency is virtually unchanged but the tank- to fuel-weight ratio is reduced by 39.1 and 27.6 percent for a design pressure of 30 and 15 psig (20.685 and 10.343 N/cm^2), respectively (in table II, compare design conditions 2 and 3 with 4 and 5). A further reduction in total tank- to fuel-weight ratio is obtained by elimination of the stringers. If the stringers are eliminated, it is necessary to increase the thickness of the tank skin for the design condition of 30 psig (20.685 N/cm^2) internal pressure; however, no increase in skin thickness over minimum gage is required for a design pressure of 15 psig (10.343 N/cm^2).

For the lower design pressure, the lightest semimonocoque tank is 32 percent heavier than the one-lobe tank (see table I); both tanks having essentially the same volumetric efficiency. For the upper-design pressure this difference increases to 80.5 percent.

CONCLUDING REMARKS

Based on the analyses performed, several designs of pressurized tanks are indicated to be feasible for the storage of liquid methane in the wings of a large supersonic transport aircraft.

1. For the typical volume envelope considered and for an internal tank pressure of 15 psig (10.343 N/cm^2), exclusive of insulation, the ratio of tank-weight to contained-fuel-weight varies from 0.024 to 0.040, and the ratio of tank fuel volume to volume available in the wing for the tank (volumetric efficiency) varies from 0.81 to 0.996. In general, the lighter tanks had the lowest volumetric efficiencies.

2. The lightest tank design for the typical void space and for a tank pressure of either 15 or 30 psig (10.343 N/cm^2 or 20.685 N/cm^2) is the single-lobe unidirectional filamentary restrained membrane tank. The pressure load on flat surfaces of the tank is carried by filaments or wires connected to opposite tank face. By arranging the filament or wires in three orthogonal directions, the volumetric efficiency can be increased from 82 to almost 100 percent; however, this gain is accompanied by an increase in tank- to contained-fuel-weight ratio of 34 to 74 percent depending on internal pressure.

3. Increasing tank pressure from 15 to 30 psig (10.343 N/cm^2 to 20.685 N/cm^2) has no effect on the weight of the conventional membrane tank because of the minimum thickness assumption. A weight increase ranging from 6 percent (single lobe-unidirectional-internally restrained membrane) to 97 percent (nonmetallic fabric filamentary restrained membrane tank) is obtained for the other tanks.

4. Sealed fabric tanks, fitted to the typical void space and employing unidirectional internal filament restraint to opposed flat faces, for a tank pressure of 15 psig (10.343 N/cm^2) have approximately the same weight and volumetric efficiency as a metal tank of the same type construction. At higher pressures the fabric tanks are indicated to be considerably heavier than corresponding metal tanks.

5. The semimonocoque type of tank construction designed for 15 psig (10.343 N/cm^2) and fitted to the typical void space results in a tank weight which is about 30 percent more than the unidirectional filamentary restrained membrane tank of the same volumetric efficiency.

6. No single tank design considered proved to be superior with respect to both volumetric efficiency and the ratio of tank weight to fuel weight. For the case where there is inadequate volume in the airplane for fuel storage and airplane redesign is necessary, detailed tank designs and aircraft range and payload analyses will be required to determine the proper compromise between tank weight and volumetric efficiency.

Lewis Research Center,
National Aeronautics and Space Administration,
Cleveland, Ohio, July 17, 1967,
720-03-51-05-22.

APPENDIX A

SYMBOLS

A	area, $in.^2$; m^2
a	tank void width, in.; m
b	one half height of ring, in.; m
C	cross section
c	membrane displacement parameter, in.; m
D	plate stiffness parameter $Et^3/12(1 - \mu^2)$, lb-in.; N - m
E	modulus of elasticity, psi, N/m^2
e	distance from centroid to neutral axis, in.; m
F	total weight of fuel contained in tank, lb; kg
H	average height of trapezoidal void or maximum tank height, in.; m
h	tank void height, in.; m
h_i	distance from centroidal axis of ring cross section to inner surface of ring, in.; m
h_o	distance from centroidal axis of ring cross section to outer surface of ring, in.; m
k	number of tank lobes
L	tank void length, in.; m
M	moment, in.-lb; m-N
Mo	statically indeterminate moment, in.-lb; m-N
N	tank height to tank width ratio, h/a
N_1	tank height to tank width ratio at large end of void
N_2	tank height to tank width ratio at small end of void
P	load, lb; N
p	pressure in tank, psi; N/m^2
p_1	component pressure balancing bending stresses
p_2	component pressure balancing membrane stresses
Q	statically indeterminate load, lb; N
q	uniform load, lb/in.; N/m
r	radius, in.; m
S	one half the distance between adjacent rings, in.; m
s	one half of side panel length, in.; m
T	total tank weight, lb; kg
t	tank skin thickness, in.; m
t_e	equivalent tie plate thickness, in.; m
U	strain energy, in.-lb; m-N
u	displacement in X direction, in.; m
V	volume, $in.^3$; m^3

v	displacement in Y direction, in.; m
w	displacement in Z direction, in.; m
w_1	displacement of side panel element at center, in.; m
X	coordinate
Y	coordinate
Z	coordinate
ϵ	strain, in./in.; m/m
η	volumetric efficiency
θ	sector angle subtended by half of tie plate, rad
λ	side panel length, in; m
μ	Poisson's ratio
ρ	tank corner radius, in.; m
σ	stress, psi; N/m^2
τ	shear stress, psi; N/m^2
ω	specific weight, $lb/in.^3$; kg/m^3

Subscripts:

a	allowable working
b	bending
c	closure material
d	drop threads
k	coating material
f	face cloth
i	inner surface of ring
l	liquid methane fuel
M	meridional
m	membrane
max	maximum
o	outer surface of ring
p	plate tie
r	ring
s	side panel
T	ties
t	tangential
w	tank material
y	yield

APPENDIX B

ANALYSIS OF CONVENTIONAL MEMBRANE TANK CHARACTERISTICS

Figure 12 shows a vertical cross section of a conventional membrane tank, situated in the storage void, where a configuration with an even number of lobes is shown on the left side and a configuration with an odd number of lobes is shown on the right side. The dimensions may be derived from the geometry of the figure.

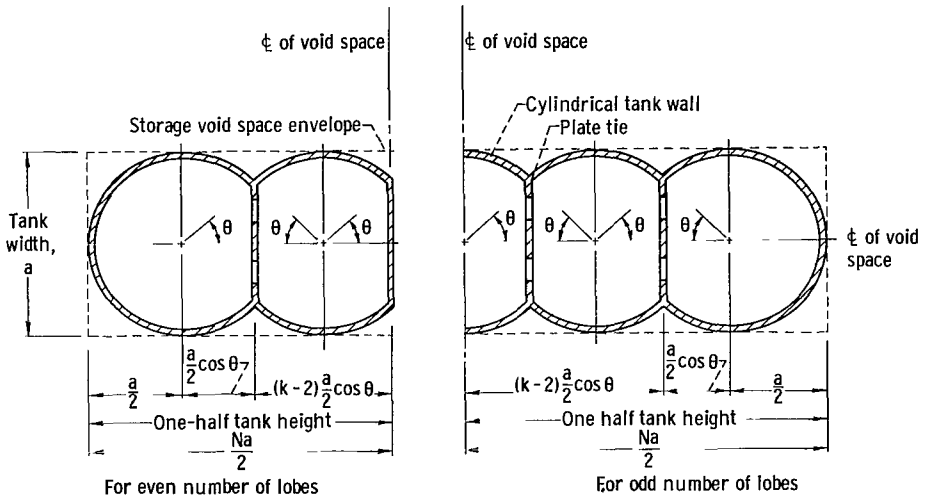

Figure 12. - Cross section through conventional membrane tank for even and odd number of lobes.

Stress in Tank Walls

The stress in the cylindrical tank walls is

$$\sigma_t = \frac{pa}{2t} \tag{B1}$$

Stress in Plate Tie

The tensile stress in the plate tie (see fig. 13) is

$$\sigma_p = \frac{pa \cos \theta}{t_e} \tag{B2}$$

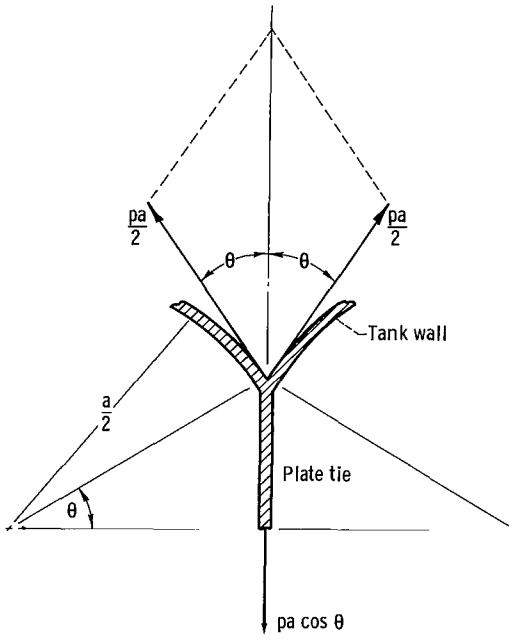

Figure 13. - Free body sketch of plate tie to tank wall connection.

From the design condition that the membrane stresses everywhere be the same, the following equation is written:

$$\sigma_t = \sigma_p \tag{B3}$$

Substituting equations (B1) and (B2) into equation (B3) yields the equivalent plate tie thickness

$$t_e = 2t \cos \theta$$

Determination of Angle θ

From figure 12, it is seen that, for all positive values of N and all integral values of $k \geq N$,

$$\cos \theta = \left(\frac{N - 1}{k - 1}\right) \tag{B4}$$

Determination of Volumetric Efficiency

$$\eta = \left(\frac{\text{Tank volume - volume of tank material}}{\text{Volume of storage void space envelope}}\right)$$

or

$$\eta = \frac{1}{N}\left(\frac{1}{4} - \frac{t}{a}\right)\left[k\pi + 2(N-1)\sqrt{1 - \left(\frac{N-1}{k-1}\right)^2} - 2(k-1)\cos^{-1}\left(\frac{N-1}{k-1}\right)\right] \tag{B5}$$

For each value of k there exists a value of N which maximizes η. The maximum values of η can be obtained by finding the roots of the equations

$$\left(\frac{\partial \eta}{\partial N}\right)_k = 0$$

where k = 1, 2, 3, 4, 5, . . ., or

$$2\left[(k-1)\cos^{-1}\left(\frac{N-1}{k-1}\right) + \sqrt{1 - \left(\frac{N-1}{k-1}\right)^2}\right] - k\pi = 0 \tag{B6}$$

Numerical values for maximum volumetric efficiency η_{max} were calculated from the preceding equations. These values are tabulated in table III and plotted in figure 9 as a function of N and k. The coefficient 1/4 - t/a is assumed equal to 1/4 since in practical applications $t/a << 1/4$.

TABLE III. - CALCULATED VALUES OF TANK HEIGHT TO TANK RATIOS FOR SELECTED NUMBER OF TANK LOBES FOR VOLUMETRIC EFFICIENCY

Number of tank lobes, k	Tank height to tank width ratio, N	Volumetric efficiency, η, percent
1	1.0000	78.5
2	1.5283	84.3
3	1.9825	87.1
4	2.3756	88.1
5	2.7349	90.1
6	3.0697	91.1
7	3.3853	91.8
8	3.6855	92.4
9	3.9730	93.5

Determination of Tank Weight to Fuel Weight Ratio

$$\frac{T}{F} = \left(\frac{\text{Total tank weight}}{\text{Contained fuel weight}}\right)$$

$$\frac{T}{F} = \left(\frac{t}{a}\right)\left(\frac{\omega_w}{\omega_l}\right)\left(\frac{1}{\frac{1}{4} - \frac{t}{a}}\right) \tag{B7}$$

For $t/a \ll 1/4$,

$$\frac{T}{F} = 4\left(\frac{t}{a}\right)\left(\frac{\omega_w}{\omega_l}\right) \tag{B8}$$

APPENDIX C

ANALYSIS OF MODIFIED SEMIMONOCOQUE TANKS

. The analysis presented herein was performed for the purpose of establishing preliminary tank designs. The scope of this investigation is limited to the study of several tank configurations, and the investigation is in sufficient detail to establish preliminary designs. Three variations of the modified semimonocoque tank design were considered, and the general features are shown in figure 3. The first configuration is a frame of intersecting stringers and rings surrounded by a leak-tight metallic skin. The second design differs from the first in that ties are added to the rings to stiffen them. The third configuration eliminates the stringers and increases the tank skin thickness in the region between the rings. Two load conditions were investigated; internal pressures of 15 psig (10.343 N/cm^2g) and 30 psig (20.685 N/cm^2).

Assumptions

The following assumptions were used in the analysis:

(1) For the tank configuration with stringers and rings the tank skin between these members is a membrane clamped at all edges.

(2) For the tank configuration without stringers the tank skin between the rings is a membrane clamped at two edges.

(3) The stringers, which are located between the rings, act as simply supported beams subjected to a uniformly distributed load.

(4) The rings are subjected to an internal uniformly distributed in plane loading.

(5) The insulation does not reinforce the tank.

(6) The allowable stress is equal to one third the yield stress of the material.

(7) The tank is fabricated from titanium.

(8) The typical volume envelope available for fuel storage is the storage void shown in figure 1.

Stress of Tank Skin

For the tank configuration with both rings and stringers the tensile stress of the tank skin, which is located between these members, is

$$\sigma = 0.396\left(\frac{p^2 E S^2}{t^2}\right)^{1/3} \tag{C1}$$

This expression for tensile stress is equation (251) of reference 3 (p. 420). In equation (C1) the tank skin is assumed to be a uniformly loaded membrane with no displacement at the boundary. As a check on the validity of this assumption, the tensile stress was calculated using large deflection plate theory, and the large deflection theory gave virtually the same results. The spacings of the rings and stringers were varied, using equation (C1), until the tensile stress in the skin became equal to the allowable stress for the material. For the configuration where the stringers were eliminated, the tensile stress in the tank skin between rings was calculated by means of the analysis in reference 4. The analysis presented in reference 4 is concerned with a uniformly loaded membrane with only the two opposite edges restrained. Using this analysis, the spacing of the rings was varied until the tensile stress of the skin became equal to the allowable stress of the skin material.

Analysis of Stringers

The stringers, which span the space between the rings, were assumed to be uniformly loaded beams, simply supported. The stress in the stringers is determined from the basic equation for bending stress in a beam. In the expression for bending stress, the stress was set equal to the allowable stress of the stringer material and the moment was determined from the design conditions. With the stress and moment terms held fixed, the cross section of the stringer was varied until a combination of centroid location and area moment of inertia was obtained which satisfied the stress equation. Since a minimum weight design is desired, the stringer with the smallest cross section, having a combination of centroid and area moment of inertia that satisfies the stress equation, was used to establish stringer size.

Analysis of Rings Without Ties

It is permissible to consider only one quadrant of the ring in the analysis since the ring has two axes of symmetry. From figure 14(a) the bending moment at any cross section C with coordinates X and Y is readily determined. From symmetry, the boundary condition at A is that the slope is zero from which an expression for Mo is determined. Using the expression for Mo, the bending moment at any point with coordinates X and Y can be obtained, and, from the general moment equation, the location and mag-

nitude of the maximum moment can be determined. If the maximum moment is located in the curved portion of the ring, the effect of ring curvature on stress distribution must be taken into account. For this case the bending stress of the ring is

$$\sigma_{b,i} = \frac{M(h_1 - e)}{A_r e r_i}$$

and

$$\sigma_{b,o} = \frac{-M(h_2 + e)}{A_r e r_o} \qquad \text{(C2)}$$

Equation (C2) is equation (212) of reference 5 (p. 365). With the bending stress of the ring set equal to the allowable stress of the ring material, and the moment set equal to its maximum value the cross section of the ring was varied until values, which satisfy the stress equation, were obtained. The ring with the smallest cross-sectional area, satisfying the stress equation, was used for the tank design. The ring at the largest end of the tank (ring with largest value of b) and the ring at the smallest end of the tank (tank with smallest value of b) were sized by the preceding analysis. The intermediate rings were sized by linear interpolation.

The flanges of the stringers and rings were checked for structural integrity against crippling by the procedure outlined in reference 6.

Analysis of Rings With Ties

The ring has two axes of symmetry; therefore, it is permissible to consider only one quadrant of the ring in the analysis.

In the analysis to follow, Mo is the redundant moment at A; Q is the redundant force at A; P is the pull of the tie, and q is a uniformly distributed in-plane loading on the ring due to tank internal pressure. The moment at any cross section of the ring between $y = [b - (a/2)]$ to $y = b$ from figure 14(b) is

$$M = Mo + (b - Y)Q - \frac{qX^2}{2} - \frac{(b - Y)^2 q}{2} \qquad \text{(C3)}$$

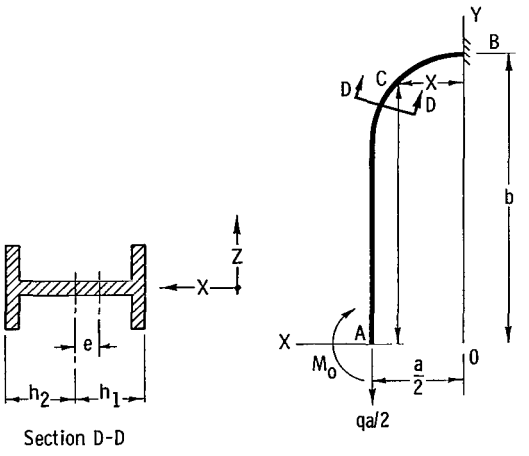

(a) Without tie.

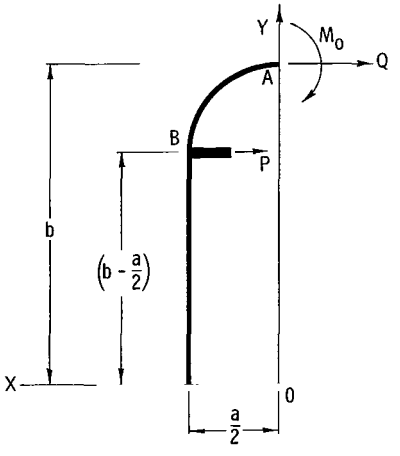

(b) With tie.

Figure 14. - Quadrant of ring.

The moment at any cross section of the ring between $y = 0$ to $y = [b - (a/2)]$ is

$$M = Mo + Q(b - Y) + P\left(b - \frac{a}{2} - Y\right) - \frac{(b - Y)^2 q}{2} - \frac{q\left(\frac{a}{2}\right)^2}{2}$$

The analysis of the rings with ties is governed by three boundary conditions: the rotation at A is zero, the deflection at A is zero, and the deflection at B is equal to the stretch of the tie or $-Pa/2A_tE$. Using the theorem of Castigliano makes possible three equations that are consistent with the boundary conditions and contain the three redundants, Mo, Q, and P. If the deflection at B is set equal to zero, rather than

$-Pa/2A_tE$, the simultaneous solution of the three boundary equations will yield the maximum value for P. If a tie size is selected in which the tensile stress is the maximum allowable working stress, very little stiffening of the ring is obtained. But, if the working tensile stress in the tie is reduced, a reduction in the maximum bending moment is obtained. This decrease in maximum bending moment results in a reduced ring weight. Total ring and tie weight was optimized by varying tie size and ring dimensions in the analytical expressions.

APPENDIX D

ANALYSIS OF FILAMENTARY RESTRAINED MEMBRANE TANK CHARACTERISTICS

Structural Considerations for Metallic Tanks

Four types of structural components are employed in the design of the filament tanks considered, namely,

(1) Wire ties

(2) End closure shells

(3) Plate ties

(4) Side panels

The wire ties and side panels are common to all five configurations considered. End closure shells exist on all configurations except the tridirectional configuration. The plate ties are found in the two- and four-lobe configurations only. These components are shown in figures 4 and 5.

Assumptions. -

(1) The material properties listed in the text apply to this appendix.

(2) The plate ties are reduced in volume by 50 percent to reduce weight and allow passages for the wire ties.

(3) The side panels can be simulated by a flat plate supported on uniformly spaced columns.

(4) The boundary conditions and deflection curves of the side panels can be expressed as trigonometric functions.

Wire ties. - The wire ties restrain the pressure load acting on the flat side panels. Based on a tie spacing of 1 inch, and an allowable working stress of 50 000 psi (34 475 N/cm^2), the cross-sectional area of each tie is

$$A_T = \frac{p}{50\ 000} \tag{D1}$$

resulting in tie diameters of 0.020 inch (0.0508 cm) for a tank pressure of 15 psig (10.34 N/cm^2gage) and 0.030 inch (0.0662 cm) for 30 psig (20.68 N/cm^2gage).

Shell end closures. - The end closures, at the ends and along the top and bottom of each tank, are analyzed as thin shells carrying membrane forces only. These closures consist of cylindrical and spherical surfaces, thus the membrane stress can be defined as

$$\sigma_M = \frac{pr}{2t}$$

and

$$\sigma_t = \frac{pr}{t} \qquad \text{(D2)}$$

for cylindrical surfaces, and

$$\sigma_M = \sigma_t = \frac{pr}{2t} \qquad \text{(D3)}$$

for spherical surfaces. Using the above equations, tank pressures of 15 and 30 psig (10.34 and 20.684 N/cm^2 gage), a tank wall thickness of 0.010 inch (0.0254 cm), and a tank width of 16 inches (40.64 cm) results in the following maximum stresses in the four configurations with shell closures:

Tank configuration	Internal tank gage pressure			
	15 psi	10.34 N/cm^2	30 psi	20.68 N/cm^2
	Maximum stresses			
	psi	N/cm^2	psi	N/cm^2
One lobe	12 000	8274	24 000	16 548
Two lobe	6 000	4137	12 000	8 274
Four lobe	3 000	2068.5	6 000	4 137
Bidirectional	12 000	8274	24 000	16 548

Plate ties. - The plate ties in the two- and four-lobe, unidirectional configurations (as shown in fig. 15) restrain the internal ends of the shell closures from moving because of forces generated by the tank internal pressure.

The closure shells at the ends, top, and bottom are restrained by common plate ties. The principal stresses in the plate ties are in-plane biaxial tensile stresses oriented in the directions of the axis of symmetry of the tank. The magnitude of the stresses for solid plate ties is equal to

$$\sigma_m = 2\frac{pr}{t} \qquad \text{(D4)}$$

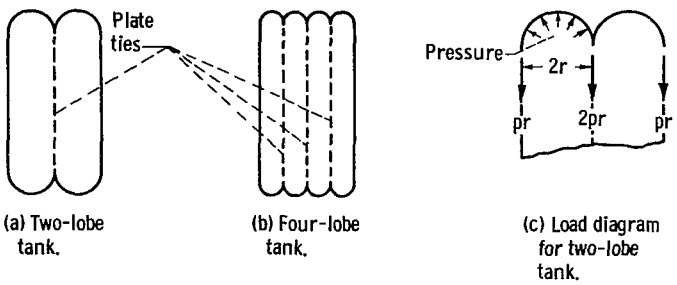

Figure 15. - Plate ties in two- and four-lobe configurations and loading diagram for two-lobe tank.

In the two configurations considered, the tie plates are perforated to reduce the weight of the plate as well as provide passages through the plates for the wire ties. In doing this, it was assumed that the cross-sectional area of the plate tie is one half that of a solid plate; therefore, the effective thickness of the plate is also reduced by 50 percent. Then equation (D4) becomes

$$\sigma_m = 4 \frac{pr}{t} \tag{D5}$$

Applying equation (D5) for an assumed minimum thickness of 0.010 inch (0.0254 cm) for the plate ties results in the following stresses:

Unidirectional tank configuration	Internal tank gage pressure			
	15 psi	10.34 N/cm^2	30 psi	20.68 N/cm^2
	Maximum stresses			
	psi	N/cm^2	psi	N/cm^2
Two lobe	24 000	16 548	48 000	33 096
Four lobe	12 000	8 274	24 000	16 548

Side panels. - The side panels are subjected to two systems of loads as shown in figure 16(a); a biaxial tensile load from the end closures and a combined bending and membrane load due to tank internal pressure.

The complete side panel is assumed to consist of a number of identical structural elements. This element, shown in figure 16(b) is assumed to be a flat plate, simply supported at the corners, subjected to a uniform pressure load and an edge tensile load. The deflections in this element will be large ($> 1/2$ t); therefore, both bending stresses and membrane stresses will be generated as a result.

An approximate analysis was conducted to obtain an indication of the stress levels.

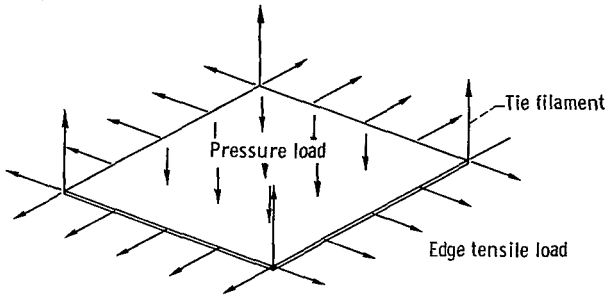

(a) Structural element of side panel with imposed loads.

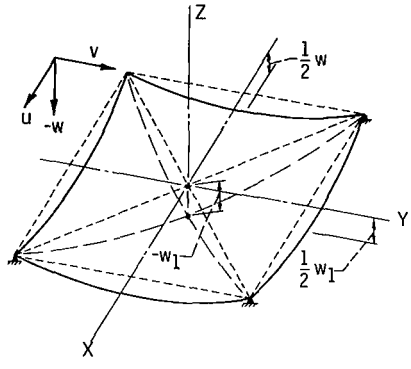

(b) Deformation of element due to imposed loads.

Figure 16. - Loading of structural element.

This analysis consisted of obtaining the stresses and deflections due to the uniform pressure load and then superimposing the edge tensile loads on these results.

In treating the side panels with respect to the lateral loads, a method outlined in reference 3 was used. This method assumes that the total pressure acting on the panel can be resolved into two components p_1 and p_2, so that

$$p = p_1 + p_2 \tag{D6}$$

The component p_1 balances the bending stresses as computed by linear plate theory and p_2 balances the membrane stresses. Expressions for the deflections and bending moment of a flat plate in terms of p_1 are available in the literature. However, the membrane solution to this particular type of problem was not found, so it was necessary to derive expressions for the deflection and stress using a strain energy method similar to that used in reference 3.

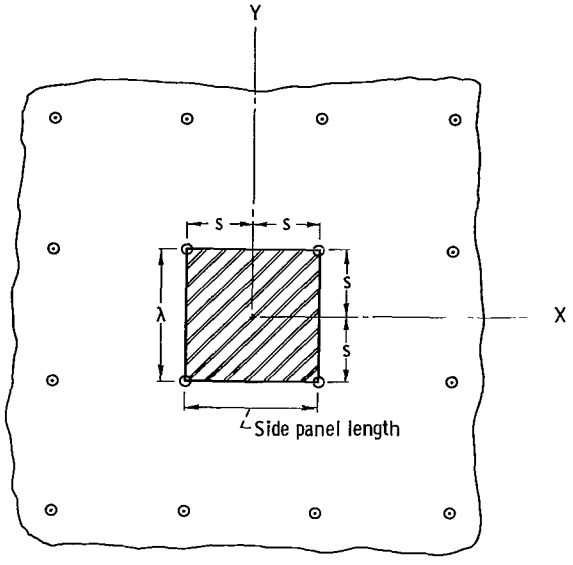

Figure 17. - Panel element in membrane of infinite extent.

The panel structural element selected for use in solving the membrane problem is shown in figure 17. The side panel is assumed to be an infinite, thin membrane of uniform thickness simply supported at uniformly spaced points. Because the panels are symmetrical, only one panel element need be looked at. The following expressions are assumed for the displacements u, v, and w, in the X, Y, and Z directions, respectively, of the middle surface.

$$u = c \sin \frac{\pi X}{s} \cos \frac{\pi Y}{2s} \tag{D7}$$

$$v = c \sin \frac{\pi Y}{s} \cos \frac{\pi X}{2s} \tag{D8}$$

$$w = \frac{1}{2} w_1 \left(\cos \frac{\pi X}{2s} + \cos \frac{\pi Y}{2s} \right) \tag{D9}$$

These expressions satisfy the following boundary conditions. At the corners

$$u = v = w = 0$$

and along the edges, away from the corners

$$u = v = 0$$

The strain energy stored in a membrane due to the stretching of its middle surface only is shown in equation (249) (p. 419 of ref. 3). The substitution of equations (D7), (D8), and (D9) into this equation, with $\mu = 0.3$, yields the following expression for strain energy:

$$U = \frac{Et}{1.82}\left(23.84\, c^2 - 3.64\, \frac{c w_1^2}{s} + 0.475\, \frac{w_1^4}{s^2}\right) \tag{D10}$$

Since no work is produced when u or v vary

$$\frac{\partial U}{\partial c} = 0 \tag{D11}$$

Applying equations (D11) to (D10) and solving for c yields

$$c = 0.0764\, \frac{w_1^2}{s} \tag{D12}$$

Substituting equation (D12) into (D10) yields

$$U = Et\left(0.2396\, \frac{w_1^4}{s^2}\right) \tag{D13}$$

From the principle of virtual displacement

$$\frac{\partial U}{\partial w_1}\Delta w_1 = \frac{1}{2}\int_{-s}^{s}\int_{-s}^{s} p\,\Delta w_1\left(\cos\frac{\pi X}{2s} + \cos\frac{\pi Y}{2s}\right)dX\,dY \tag{D14}$$

Applying equations (D14) to (D13) and solving for w_1 yields

$$w_1 = 1.39\, s\, \sqrt[3]{\frac{ps}{Et}} \tag{D15}$$

The membrane stress in the middle surface is obtained from the tensile strains of this surface.

$$\sigma_m = \frac{E}{1 - \mu} \epsilon_X \tag{D16}$$

$$\epsilon_X = \epsilon_Y = \frac{\partial u}{\partial X} = \frac{\partial v}{\partial Y} = \frac{\pi c}{s} \tag{D17}$$

Using equations (D16), (D17), (D12), and (D15) results in

$$\sigma_m = 0.343 \frac{E w_1^2}{s^2} = 0.66 \sqrt[3]{\frac{p^2 E s^2}{t^2}} \tag{D18}$$

With equations (D15), (D18), and the following flat plate formulas

$$w_1 = 0.00581 \frac{p\lambda^4}{D} \tag{D19}$$

$$\sigma_b = \frac{6}{t^2} (0.0331) p\lambda^2 \tag{D20}$$

an approximation of the stresses and deflections in the side panel element can be obtained. Equations (D19) and (D20) are applicable to a continuous flat plate supported by uniformly spaced columns. Using equation (D15) for p_2 and equation (D19) for p_1 in equation (D6) results in the following expression:

$$p = \frac{w_1 D}{0.00581\ \lambda^4} + \frac{w_1^3 E t}{(1.39)^3 s^4} \tag{D21}$$

Using $p = 15$ and $p = 30$ psig (10.34 and 20.68 N/cm^2, respectively,

Side panel length, λ, in. (cm)	1(2.54)
Modulus of elasticity, E, psi (N/cm^2)	17×10^6(72×10^6)
Tank skin thickness, t, in. (cm)	0.010(0.0254)
One half of side panel length, s, in. (cm)	1/2(1.27)
Poisson's ratio, μ	0.3

the following displacements at the center of the panel are obtained: For 15 psig (10.34 N/cm^2), w_1 = 0.0209 inch (0.0531 cm) and for 30 psig (20.68 N/cm^2), w_1 = 0.0280 inch (0.0711 cm). These results are used with equations (D15) and (D18) to (D20) to obtain the stresses at the center of the panel element as follows:

Stress	Internal tank gage pressure			
	15 psi	10.34 N/cm^2	30 psi	20.68 N/cm^2
	Stress at center of panel element			
	psi	N/cm^2	psi	N/cm^2
Bending	11 130	7 674	14 900	10 274
Membrane	10 390	7 164	18 400	12 687
Total	21 420	14 838	33 300	22 961

These stresses combined with the tensile edge stresses give an approximation of the total stress in the panels. The maximum stress occurs in the one-lobe configuration and is equal to about 57 000 psi (39 800 N/cm^2) in the outer fibers of the panel (dry side). The middle plane stresses are 33 300 psi (22 961 N/cm^2), and the outer fibers on the fuel side are at 28 500 psi (16 250 N/cm^2).

Tank Characteristics

The tank characteristics investigated, tank volume, tank weight, volumetric efficiency and tank- to fuel-weight ratio, are obtained directly from the tank shape and its dimensions. The equations used in this analysis are as follows:

Tank volumes. -

One-lobe tank:

$$V_{tank} = \frac{\pi}{4} a^2 \left(L + H - \frac{4}{3} a\right) + aHL - a^2(L + H - a) \tag{D22}$$

Two-lobe tank:

$$V_{tank} = \frac{\pi}{8} a^2 \left(L + H - \frac{2}{3} a\right) + aHL - \frac{1}{2} a^2 \left(H + L - \frac{1}{2} a\right) \tag{D23}$$

Four-lobe tank:

$$V_{tank} = \frac{\pi}{16} a^2 \left(L + H - \frac{1}{3} a\right) + aHL - \frac{1}{4} a^2 \left(L + H - \frac{1}{4} a\right) \tag{D24}$$

Bidirectional tank:

$$V_{tank} = \frac{\pi}{4} a^2 \left(H - \frac{1}{3} a\right) + aHL - a^2 H \tag{D25}$$

Tridirectional tank:

$$V_{tank} = aHL - \rho^2 (4 - \pi)(L + H + a) - 3\, aHLA_T \tag{D26}$$

where ρ is the corner radius on the tank (1 in. assumed for calculations).

Fuel weights. - The fuel weight equation for all tanks is

$$F = \omega_l V_{tank} \tag{D27}$$

Volumetric efficiency. -

$$\eta = \frac{V_{tank}}{V_{void}} \tag{D28}$$

Tank weights. -

One-lobe tank:

$$T = \omega_w \left\{ t \left[\pi a(L + H - a) + 2HL - 2a(L + H - a) \right] + \left[aHL - a^2 (L + H - a) \right] A_T \right\} \tag{D29}$$

Two-lobe tank:

$$T = \omega_w \left(t \left\{ \pi a \left(L + H - \frac{1}{4} a\right) + 2HL - a \left(L + H - \frac{1}{2} a\right) + \frac{1}{2} \left[HL - \frac{1}{2} a \left(H + L - \frac{a}{2}\right) \right] \right\} + \left[aHL - \frac{1}{2} a^2 \left(L + H - \frac{a}{2}\right) \right] A_T \right) \tag{D30}$$

Four-lobe tank:

$$T = \omega_w \left(t \left\{ \pi a \left(L + H - \frac{1}{4} a \right) + 2HL - \frac{1}{2} a \left(L + H - \frac{1}{4} a \right) + \frac{3}{2} \left[HL - \frac{1}{4} a \left(L + H - \frac{1}{4} a \right) \right] \right\} + \left[aHL - \frac{1}{4} a^2 \left(L + H - \frac{1}{4} a \right) \right] A_T \right) \quad \text{(D31)}$$

Bidirectional tank:

$$T = \omega_w \left\{ t \left[\pi aH + 2(H + a)(L - a) \right] + 2(aHL - a^2 H) A_T \right\} \quad \text{(D32)}$$

Tridirectional tank:

$$T = \omega_w \left[2t(aL + aH + HL) + 3\, aHLA_T \right] \quad \text{(D33)}$$

One-lobe fabric tank:

$$T = a \left\{ 6\omega_f t_f \left[HL - a(L + H) + a^2 + 2\left(\frac{\pi}{2} a + 2 \right)(L + H - 2a) \right] \right\} + \left(a\omega_T + 3.856 \times 10^{-5} \right) \left[HL - a(L + H) + a^2 \right] \quad \text{(D34a)}$$

Equation (D34a) is an empirical equation developed by a manufacturer of this type of tank. The expression in braces is the weight of a tank 1 inch in width (2.54 cm) and has units of pounds per inch (kg/m). For SI units, equation (D34a) becomes

$$T = a \left\{ 6\omega_f t_f \left[HL - a(L + H) + a^2 + \left(\frac{\pi}{2} a + 2 \right)(L + H - 2a)2 \right] \right\} + \left(a\omega_T + 2.712 \times 10^{-2} \right) \left[HL - a(L + H) + a^2 \right] \quad \text{(D34b)}$$

APPENDIX E

ANALYSIS OF THREE-LOBE CONVENTIONAL MEMBRANE TANK CHARACTERISTICS

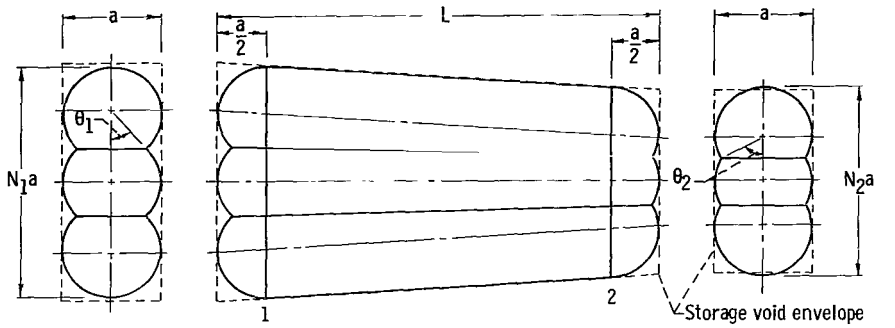

Figure 18. - Three-lobe conventional membrane tank for typical shape of storage void in wing.

From figure 18 the total tank volume is

$$\text{Tank volume} \approx (L - a)\frac{a^2}{8}\left\{6\pi - 4\left[\cos^{-1}\left(\frac{N_1 - 1}{2}\right) + \cos^{-1}\left(\frac{N_2 - 1}{2}\right)\right] + (N_1 - 1)\sqrt{3 + N_1(2 - N_1)} + (N_2 - 1)\sqrt{3 + N_2(2 - N_2)}\right\}$$

$$+ \frac{\pi a^3}{12}\left\{6 - \frac{3}{4}\left[(3 - N_1)^2 + (3 - N_2)^2\right] + \frac{1}{8}\left[(3 - N_1)^3 - (3 - N_2)^3\right]\right\} \qquad \text{(E1)}$$

The volume enclosed by the storage void envelope is

$$\text{Void volume} = \frac{1}{2}a^2L(N_1 + N_2) \qquad \text{(E2)}$$

The volumetric efficiency is

$$\eta = \frac{\text{Total tank volume}}{\text{Void volume}} \qquad \text{(E3)}$$

The total tank weight is

$$T = \frac{\pi a^2 \omega_w t}{2}(N_1 + N_2) + \frac{atL\omega_w}{2}\left\{6\pi - 4\left[\cos^{-1}\left(\frac{N_1 - 1}{2}\right) + \cos^{-1}\left(\frac{N_2 - 1}{2}\right)\right]\right.$$

$$\left. + (N_1 - 1)\sqrt{3 + N_1(2 - N_1)} + (N_2 - 1)\sqrt{3 + N_2(2 - N_2)}\right\} \qquad \text{(E4)}$$

The tank weight to fuel weight ratio is

$$\frac{T}{F} = \frac{\text{Tank total weight}}{(\text{Tank total volume}) \times \omega_l} \qquad \text{(E5)}$$

REFERENCES

1. Whitlow, John B., Jr.; Eisenberg, Joseph D.; and Shovlin, Michael D.: Potential of Liquid-Methane Fuel for Mach-3 Commercial Supersonic Transports. NASA TN D-3471, 1966.

2. Sanz, M. C.; and Castelfranco, J.: Aircraft Insulated Fuel Tank. U S. Patent No. 2,676,773, Jan. 8, 1951.

3. Timoshenko, S.; and Woinowsky-Krieger, S.: Theory of Plates and Shells. Second ed., McGraw-Hill Book Co., Inc., 1959.

4. Wilson, P. E.; and Slick, E. M.: Large Deflection of a Uniformly Loaded Membrane Strip. Rep. No. GD/A-DDG64-008, General Dynamics/Astronautics, May 1, 1964.

5. Timoshenko, Stephen: Strength of Materials. Vol. I. Third ed., D. Van Nostrand Co., Inc., 1955.

6. Martinelli, J. A.: How to Determine Critical Crippling Stress of Formed Sheet-Metal Sections. Machine Des., vol. 38, no. 18, Aug. 4, 1966, pp. 163-167.

NASA-Langley, 1967 —— 32 E-3893

"The aeronautical and space activities of the United States shall be conducted so as to contribute . . . to the expansion of human knowledge of phenomena in the atmosphere and space. The Administration shall provide for the widest practicable and appropriate dissemination of information concerning its activities and the results thereof."

—NATIONAL AERONAUTICS AND SPACE ACT OF 1958

NASA SCIENTIFIC AND TECHNICAL PUBLICATIONS

TECHNICAL REPORTS: Scientific and technical information considered important, complete, and a lasting contribution to existing knowledge.

TECHNICAL NOTES: Information less broad in scope but nevertheless of importance as a contribution to existing knowledge.

TECHNICAL MEMORANDUMS: Information receiving limited distribution because of preliminary data, security classification, or other reasons.

CONTRACTOR REPORTS: Scientific and technical information generated under a NASA contract or grant and considered an important contribution to existing knowledge.

TECHNICAL TRANSLATIONS: Information published in a foreign language considered to merit NASA distribution in English.

SPECIAL PUBLICATIONS: Information derived from or of value to NASA activities. Publications include conference proceedings, monographs, data compilations, handbooks, sourcebooks, and special bibliographies.

TECHNOLOGY UTILIZATION PUBLICATIONS: Information on technology used by NASA that may be of particular interest in commercial and other non-aerospace applications. Publications include Tech Briefs, Technology Utilization Reports and Notes, and Technology Surveys.

Details on the availability of these publications may be obtained from:

SCIENTIFIC AND TECHNICAL INFORMATION DIVISION

NATIONAL AERONAUTICS AND SPACE ADMINISTRATION

Washington, D.C. 20546